

HORIZONTAL AND VERTICAL EMITTANCE MEASUREMENTS OF THE ADVANCED PHOTON SOURCE BOOSTER SYNCHROTRON BEAM AT HIGH CHARGE*

K. P. Wootton[†], W. J. Berg, J. R. Calvey, K. C. Harkay, A. Xiao, B. X. Yang
Argonne National Laboratory, Lemont, IL 60439, USA
A. H. Lumpkin, C.-Y. Yao, Argonne Associate of Global Empire, LLC,
Argonne National Laboratory, Lemont, IL 60439, USA

Abstract

In order to maximise the injection efficiency from the booster synchrotron into the proposed Advanced Photon Source Upgrade storage ring, beam-based optimisation of the booster electron optical lattice is anticipated. In the present work, we present non-destructive beam size and emittance measurements using the booster synchrotron light monitor and destructive quadrupole scan emittance measurements in the booster to storage ring transport line. Destructive measurements are performed with a 0.1 mm thickness Cerium-doped Yttrium Aluminium Garnet screen. In order to characterise performance, both the beam energy at extraction (5, 6 and 7 GeV) and the bunch charge are varied.

INTRODUCTION

The Advanced Photon Source Upgrade (APS-U) is a project to convert the existing facility to a high brilliance diffraction limited electron storage ring light source [1]. A distinguishing feature of multibend achromat lattices for diffraction limited storage rings is that the dynamic aperture is small enough that on-axis injection (rather than off-axis accumulation) becomes desirable [2, 3]. As a result, a high charge single bunch injector is an important feature of the design of the APS-U [4–7] and also the High Energy Photon Source [8, 9].

In order to efficiently inject into the APS-U storage ring, it is desired to monitor and optimise in particular the horizontal emittance of the high charge electron bunch extracted from the booster synchrotron. We consider several established diagnostics to measure the horizontal and vertical emittances in the booster [10]. For a non-destructive measurement of the stored beam in the booster, an optical synchrotron light monitor (SLM) was used [11, 12]. Destructive quadrupole scan emittance measurements of the electron beam emittance can be performed in the booster to storage ring transport line. The diagnostics used in this study are illustrated schematically in Fig. 1.

QUADRUPOLE EMITTANCE SCANS

Consider the beamline in Fig. 2. The beam encounters a quadrupole of length l_q and strength k that focusses the

beam in one dimension. The beam then traverses a drift of length d and is imaged on a screen.

The emittance is given by [13]:

$$\varepsilon = \sqrt{\Sigma_{0,11}\Sigma_{0,22} - \Sigma_{0,12}^2}, \quad (1)$$

The beam size at the screen ($\Sigma_{1,ij}$) can be expressed in terms of the beam size at the entrance of the quadrupole ($\Sigma_{0,kl}$) by [13]:

$$\Sigma_{1,11}(k) = \left(d^2 l_q^2 \Sigma_{0,11}\right) k^2 + \left(-2d l_q \Sigma_{0,11} - 2d^2 l_q \Sigma_{0,12}\right) k + \left(\Sigma_{0,11} + 2d \Sigma_{0,12} + d^2 \Sigma_{0,22}\right). \quad (2)$$

Uncertainties in the fitted parameters were determined by propagation of uncertainty. We follow an approach similar to Refs. [14, 15]. For a general parameter g , the uncertainty σ_g can be expressed by [15]:

$$\sigma_g^2 = \sum_{i=1}^n \left(\frac{\partial g}{\partial x_i}\right)^2 \sigma_{x_i}^2 + \sum_{i=1}^j \sum_{j=1, j \neq i}^j \left(\frac{\partial g}{\partial x_i}\right) \left(\frac{\partial g}{\partial x_j}\right) C(i, j) \quad (3)$$

where $\sigma_{x_i}^2$ are the variances of the fitted parameters x_i , and C is the covariance between them, which are determined when fitting Eq. (2) to measured beam moments. Because the terms $\Sigma_{0,ij}$ are not independent of one another, we partially differentiate the emittance with respect to each term.

$$\frac{\partial \varepsilon}{\partial \Sigma_{0,11}} = \frac{-\Sigma_{0,11} d^{-2} + \Sigma_{0,22} + 2\Sigma_{0,12} d^{-1}}{2\sqrt{\Sigma_{0,11}\Sigma_{0,22} - \Sigma_{0,12}^2}}, \quad (4)$$

$$\frac{\partial \varepsilon}{\partial \Sigma_{0,12}} = \frac{-2\Sigma_{0,11} d^{-1} - d\Sigma_{0,22} - 2\Sigma_{0,12}}{2\sqrt{\Sigma_{0,11}\Sigma_{0,22} - \Sigma_{0,12}^2}}, \quad (5)$$

$$\frac{\partial \varepsilon}{\partial \Sigma_{0,22}} = \frac{\Sigma_{0,11} - d^2 \Sigma_{0,22} + d \Sigma_{0,12}}{2\sqrt{\Sigma_{0,11}\Sigma_{0,22} - \Sigma_{0,12}^2}}. \quad (6)$$

The lattice parameters at the quadrupole are given by:

$$\beta(s) = \Sigma_{0,11} (\Sigma_{0,11}\Sigma_{0,22} - \Sigma_{0,12})^{-1/2}, \quad (7)$$

$$\alpha(s) = -\Sigma_{0,12} (\Sigma_{0,11}\Sigma_{0,22} - \Sigma_{0,12})^{-1/2}, \quad (8)$$

$$\gamma(s) = \Sigma_{0,22} (\Sigma_{0,11}\Sigma_{0,22} - \Sigma_{0,12})^{-1/2}. \quad (9)$$

* Work supported by the U.S. Department of Energy, Office of Science, Office of Basic Energy Sciences, under Contract No. DE-AC02-06CH11357.

[†] kwootton@anl.gov

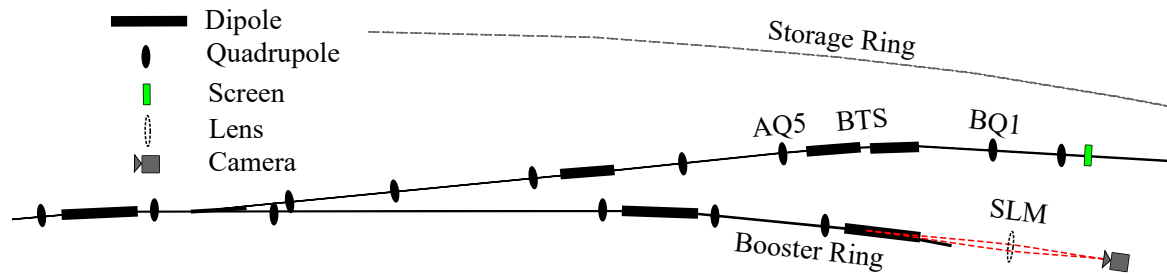


Figure 1: Booster emittance diagnostics layout. The source point for the synchrotron light monitor (SLM) is within a bending magnet in the booster ring. For quadrupole scan emittance measurements in the Booster-to-Storage Ring (BTS) transport line, the nearest upstream horizontally focussing quadrupole is BQ1, and the nearest useable vertically focussing quadrupole is AQ5.

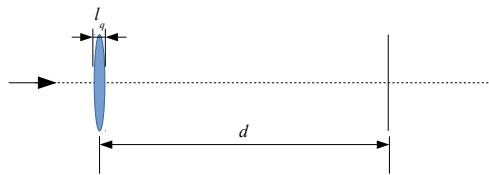


Figure 2: Conceptual overview of beamline. The beam encounters a quadrupole of length l_q and strength k that focusses the beam in one dimension. The beam then traverses a drift of length d and is imaged on a screen.

Quadrupole Scan Hardware

In January of 2019 the old Chromox scintillator screen at this location was replaced with a 0.1 mm thick Cerium-doped Yttrium Aluminium Garnet (Ce:YAG) scintillator [16].

For the quadrupole scans, an analogue camera and frame grabber is used to acquire and digitise images of the beam. An image of the beam at the horizontal waist is given in Fig. 3 and the vertical waist in Fig. 4. For the optical system and digitising frame grabber used at the BTS flag station, the effective pixel size is $115.9 \mu\text{m pix}^{-1}$ in the horizontal and $90.9 \mu\text{m pix}^{-1}$ in the vertical direction.

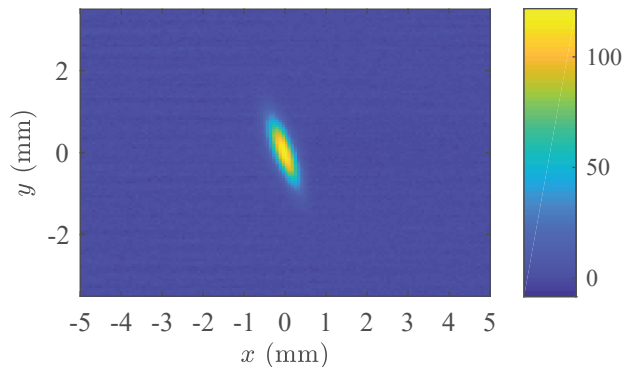


Figure 3: Measured electron beam distribution imaged on a YAG screen, at the horizontal waist of a horizontal emittance quadrupole scan.

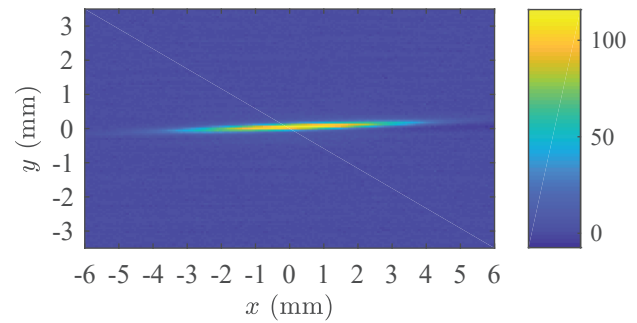


Figure 4: Measured electron beam distribution imaged on a YAG screen, at the vertical waist of a vertical emittance quadrupole scan.

The quadrupole power supplies in the BTS transport line are unipolar. For the horizontal emittance measurement, the excitation current of the nearest upstream horizontally focussing quadrupole (BTS:BQ1) was scanned. The distance separating BQ1 and the Ce:YAG screen is 3.77 m. A quadrupole scan of the horizontal emittance is illustrated in Fig. 5.

For the vertical emittance measurement, the excitation current of the nearest upstream vertically focussing quadrupole (BTS:AQ5) was scanned. The distance separating AQ5 and the Ce:YAG screen is 11.97 m. Although the lattice between BTS:AQ5 and the YAG screen is not a drift (there is a horizontally-deflecting bending magnet between them), we make the simplifying assumption that the vertical dispersion is small along the BTS line and treat the separation of the quadrupole and YAG screen as a drift in the vertical axis. A quadrupole scan of the vertical emittance is illustrated in Fig. 6.

SYNCHROTRON LIGHT MONITOR

The electron beam is imaged using synchrotron light emitted at one of the booster synchrotron bending magnets [11, 12]. The electron beam optical functions of the booster synchrotron FODO lattice at the location of the source point of the synchrotron light monitor are summarised in Table 1.

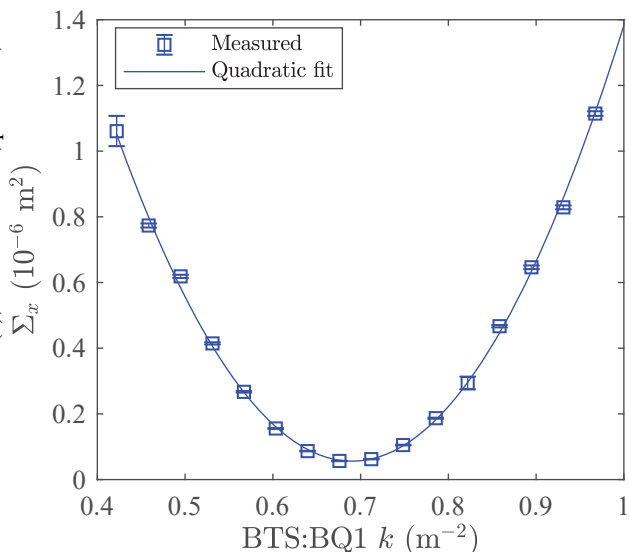


Figure 5: Measured electron beam horizontal moment with variation of vertically focussing quadrupole BQ1 excitation current.

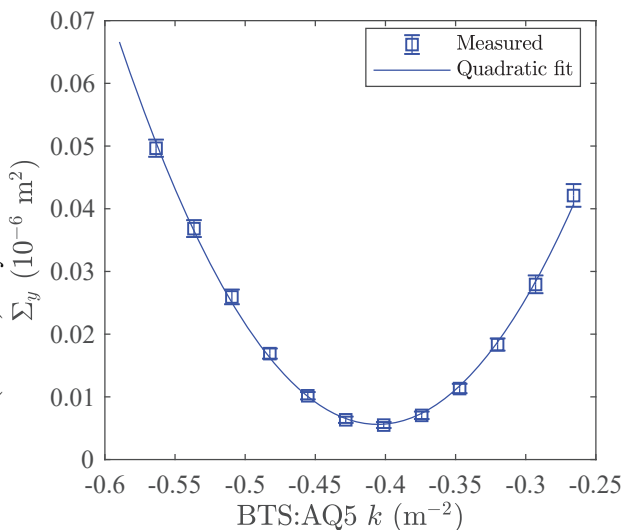


Figure 6: Measured electron beam vertical moment with variation of vertically focussing quadrupole AQ5 excitation current.

Table 1: Nominal Booster Electron Optical Lattice Parameters at Synchrotron Light Monitor Source Point

Lattice parameter	Value	Units
$\beta_x(s)$	4.18	m
$\eta_x(s)$	0.48	m
$\beta_y(s)$	11.83	m
$\eta_y(s)$	0.00	m

Synchrotron Light Monitor Hardware

The synchrotron light monitor is an optical beamline [11, 12, 17, 18]. The electron beam distribution is imaged using

a single lens. Optical components of the synchrotron light monitor beamline are summarised in Table 2.

The optical magnification of the synchrotron light monitor beamline is 0.577. The camera used is a Point Grey Research Grasshopper3 (greyscale sensor). With a sensor pixel size of $5.86 \mu\text{m}$, this gives an effective pixel size at the electron beam source point of $10.15 \mu\text{pix}^{-1}$.

Table 2: Optical Components of Synchrotron Light Monitor, and Distance s from Electron Beam Source [18]

Component	s (m)
Electron beam source	0.000
$f = +2.0$ m lens (Melles Griot LAO379)	5.466
Neutral density filters (0.0-6.0 OD)	8.420
450 nm filter, 10 nm bandpass	8.520
CMOS Camera (Point Grey Grasshopper3)	8.620

Results

An example image of the electron beam distribution imaged using the synchrotron light monitor is given in Fig. 7. Varying the camera trigger, the electron beam distribution was acquired at different times during the acceleration ramp, for different bunch charges. This is plotted in Fig. 8.

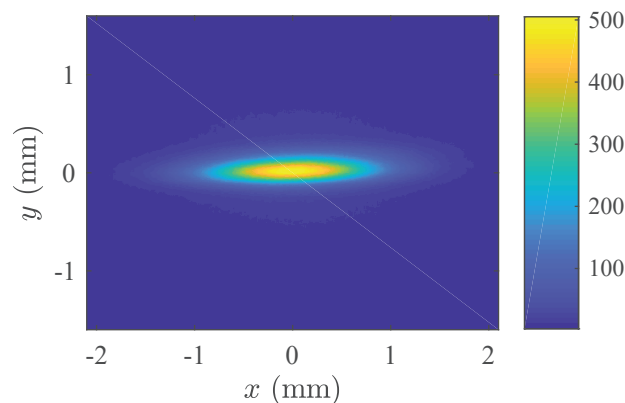


Figure 7: Electron beam image measured in the booster synchrotron ring using the synchrotron light monitor at 7 GeV and 11 nC.

SUMMARY

A summary of horizontal electron beam emittances at 5, 6 and 7 GeV is presented in Fig. 9. Effectively, the measured horizontal emittance is increasing with the excitation from synchrotron radiation as the energy increases. Similarly, a summary of vertical electron beam emittances at 5, 6 and 7 GeV is presented in Fig. 10. Effectively, the measured vertical emittance was not observed to change with energy.

We have measured the transverse emittance of high charge beams in the booster synchrotron using optical synchrotron radiation. We have not yet measured the emittance of beams extracted at such high charge in the BTS transport line. In

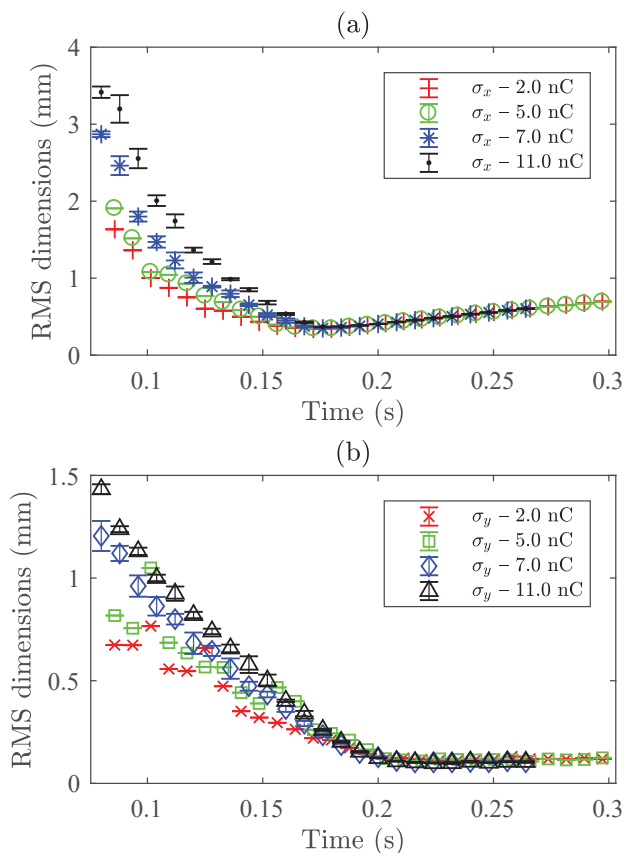


Figure 8: Measured booster synchrotron light monitor scan of electron beam horizontal (a) and vertical (b) size during the acceleration ramp. Multiple injected charges were measured between 2 and 11 nC. Essentially, once there is sufficient synchrotron radiation damping, the beam size damps to equilibrium independent of the injected charge within this range.

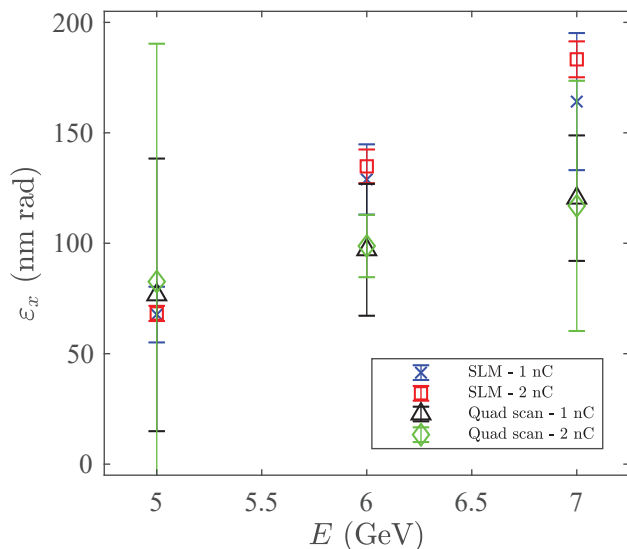


Figure 9: Summary of horizontal emittance measurements at different energies and charges. Effectively, the measured emittance is increasing with the excitation from synchrotron radiation as the energy increases.

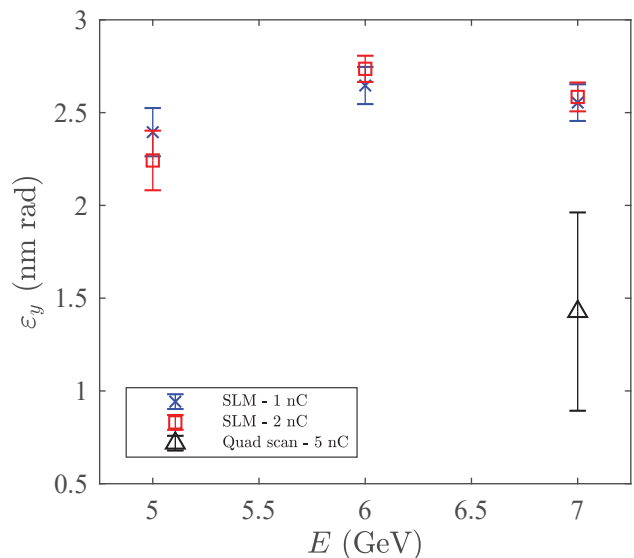


Figure 10: Summary of vertical emittance measurements at different energies and charges. Effectively, the measured emittance is not changing with energy.

order to measure the emittance in the BTS transport line using quadrupole scans at higher charge, new radiological surveys will be performed.

CONCLUSION

Operation of the booster synchrotron at bunch charges exceeding 10 nC will be important for several proposed electron beam filling patterns of the APS-U. For efficient beam transport and acceptance into the APS-U storage ring, low transverse emittance is desired. In the present work, we have measured electron beam size and emittance in the booster synchrotron using a synchrotron light monitor and quadrupole scans. We have not observed a significant increase in transverse emittance with injected bunch charge.

ACKNOWLEDGEMENTS

The submitted manuscript has been created by UChicago Argonne, LLC, Operator of Argonne National Laboratory (“Argonne”). Argonne, a U.S. Department of Energy Office of Science Laboratory, is operated under Contract No. DE-AC02-06CH11357. The U.S. Government retains for itself, and others acting on its behalf, a paid-up nonexclusive, irrevocable worldwide license in said article to reproduce, prepare derivative works, distribute copies to the public, and perform publicly and display publicly, by or on behalf of the Government. The Department of Energy will provide public access to these results of federally sponsored research in accordance with the DOE Public Access Plan.

<http://energy.gov/downloads/doe-public-access-plan>

REFERENCES

- [1] T. E. Fornek, “Advanced Photon Source Upgrade Project Final Design Report”, Argonne National Laboratory, Lemont,

- IL, USA, Rep. APSU-2.01-RPT-003, May 2019.
doi:10.2172/1543138
- [2] R. Abela, W. Joho, P. Marchand, S. V. Milton, and L. Z. Rivkin, “Design Considerations for a Swiss Light Source (SLS)”, in *Proc. 3rd European Particle Accelerator Conf. (EPAC’92)*, Berlin, Germany, Mar. 1992, pp. 486–489.
- [3] L. Emery and M. Borland, “Possible Long-Term Improvements to the Advanced Photon Source”, in *Proc. 20th Particle Accelerator Conf. (PAC’03)*, Portland, OR, USA, May 2003, paper TOPA014, pp. 256–258.
doi:10.1109/PAC.2003.1288895
- [4] A. Xiao, M. Borland, and C. Yao, “On-axis Injection Scheme for Ultra-Low-Emittance Light Sources”, in *Proc. North American Particle Accelerator Conf. (NAPAC’13)*, Pasadena, CA, USA, Sep.-Oct. 2013, paper WEPSM13, pp. 1076–1078.
- [5] A. Xiao and M. Borland, “Transport Line Design and Injection Configuration Optimization for the Advanced Photon Source Upgrade”, in *Proc. 9th Int. Particle Accelerator Conf. (IPAC’18)*, Vancouver, Canada, Apr.-May 2018, pp. 1287–1289.
doi:10.18429/JACoW-IPAC2018-TUPMF017
- [6] M. Borland *et al.*, “The Upgrade of the Advanced Photon Source”, in *Proc. 9th Int. Particle Accelerator Conf. (IPAC’18)*, Vancouver, Canada, Apr.-May 2018, pp. 2872–2877.
doi:10.18429/JACoW-IPAC2018-THXGBD1
- [7] K. C. Harkay *et al.*, “High-Charge Injector for on-Axis Injection Into A High-Performance Storage Ring Light Source”, in *Proc. 10th Int. Particle Accelerator Conf. (IPAC’19)*, Melbourne, Australia, May 2019, pp. 3423–3426.
doi:10.18429/JACoW-IPAC2019-THYYPLM3
- [8] Z. Duan *et al.*, “The Swap-Out Injection Scheme for the High Energy Photon Source”, in *Proc. 9th Int. Particle Accelerator Conf. (IPAC’18)*, Vancouver, Canada, Apr.-May 2018, pp. 4178–4181.
doi:10.18429/JACoW-IPAC2018-THPMF052
- [9] S. Jiang, and G. Xu, “On-axis injection scheme based on a triple-frequency rf system for diffraction-limited storage rings”, *Phys. Rev. Accel. Beams*, vol. 21, p. 110701, 2018.
doi:10.1103/PhysRevAccelBeams.21.110701
- [10] B. Yang, “Optical System Design for High-Energy Particle Beam Diagnostics”, *AIP Conf. Proc.*, vol. 648, pp. 59–78, 2002.
doi:10.1063/1.1524392
- [11] A. Lumpkin, *et al.*, “Initial diagnostics commissioning results for the Advanced Photon Source (APS)”, in *Proc. 16th Particle Accelerator Conf. (PAC’95)*, Dallas, TX, USA, May 1995, paper MPQ10, pp. 2473–2475.
doi:10.1109/PAC.1995.505588
- [12] A. Lumpkin, and B. Yang, “Status of the synchrotron radiation monitors for the APS facility rings”, in *Proc. 16th Particle Accelerator Conf. (PAC’95)*, Dallas, TX, USA, May 1995, paper MPQ09, pp. 2470–2472.
doi:10.1109/PAC.1995.505587
- [13] H. Wiedemann, “Particle Beams and Phase Space”, in *Particle Accelerator Physics*, 4th Edition. Switzerland: Springer International Publishing, 2015, pp. 213–251.
doi:10.1007/978-3-319-18317-6_8
- [14] K. D. Jacobs, J. B. Flanz, and T. Russ, “Emittance measurements at the Bates linac”, in *Proc. 1989 IEEE Particle Accelerator Conf.*, IEEE Publishing, Piscataway, NJ, USA, vol. 3, pp. 1526–1528, 1989.
doi:10.1109/PAC.1989.73501
- [15] F. Lühl, “Measurements of the transverse emittance at the VUV-FEL”, Diploma thesis, University of Hamburg, Hamburg, Germany, July 2005.
doi:10.3204/DESY-THESIS-2005-014
- [16] A. H. Lumpkin, W. Berg, J. C. Dooling, K. P. Wootton, and C. Yao, “Proposed Enhanced Imaging Station in the 6-GeV Booster-to-Storage Ring Transport Line for APS Upgrade”, presented at the North American Particle Accelerator Conf. (NAPAC’19), Lansing, MI, USA, Sep. 2019, paper TUPLE11.
- [17] A. Lumpkin, *et al.*, “Initial diagnostics commissioning results for the APS injector subsystems”, *AIP Conf. Proc.*, vol. 333, pp. 181–187, 1995.
doi:10.1063/1.48068
- [18] B. Yang, private communication, Aug. 2017.